

Computation and Design of Detailed Sizing of Stator Slot Types Utilized in Axial Flux Permanent Magnet Machines

Thanh Nguyen Vu *[‡] , Khoi Nguyen Trong ** 

*Department of Electrical Engineering, School of Electronic and Electrical Engineering, Hanoi University of Science and Technology, No. 1 Dai Co Viet Street, Bach Khoa ward, Hai Ba Trung district, Hanoi City, Vietnam

**Department of Electrical Engineering, School of Electronic and Electrical Engineering, Hanoi University of Science and Technology, No. 1 Dai Co Viet Street, Bach Khoa ward, Hai Ba Trung district, Hanoi City, Vietnam

(thanh.nguyenvu@hust.edu.vn, khoi.nt181185@sis.hust.edu.vn)

[‡]Corresponding Author; First Author, Postal address, Tel: +84 912 353 376,

thanh.nguyenvu@hust.edu.vn

Received: 13.06.2023 Accepted: 18.07.2023

Abstract- One of the critical processes is the detailed design computation of the stator slot size of axial flux permanent magnet machines (AFPMS), which has a significant impact on their performance, particularly their magnetic field distribution. An algorithm for the precise design of the stator slot sizing is provided in this study. The algorithm is developed by step-by-step calculation analytics. The authors' main contribution is to give formulas for computing the H_{s2} slot height for each type of slot. The authors of the study make certain recommendations, and one of those recommendations is that the investigation of the flux density on the stator tooth be accomplished through simulation software using the finite element method. This is done so that the authors' recommendations may be proven. The analytic calculation makes the tooth flux density assumption, and the results reveal that the variation from this assumption is not very significant at all.

Keywords Stator slot sizing, AFPM, AFPMG, tooth flux density.

1. Introduction

AFPM devices are classified as disc machines [3]. It is extensively used in machinery equipment requiring high torque at low speed, particularly gearless direct drive equipment. According to [4], up to 69.05% of announcements about electric machines in the past five years have been about AFPM machines. It demonstrates that such a type of electric machine is currently receiving a great deal of interest from scientists around the world.

In terms of structure, AFPM machines are typically divided into a total of four different types [1, 4, 5], including: single-sided machine (SSM), double-sided machines with double-rotor (TORUS), double-sided machines with double-stator (AFIR), and multi-disc machines with multi-rotor, multi-stator (MRMS). These four types are further separated into the slotted stator and slotless stator groups. The

electromagnetic design of the slotted stator AFPM machine progresses through several stages, the first of which involves determining the main dimensions listed in "Table 1."

Table 1. Main dimensions of AFPM [6]

Main dimensions
Outer diameter (D_o)
Diameter ratio (k_d)
Air-gap (g)
Axial length of the stator (L_s)
Axial length of the rotor (L_r)
Axial length of permanent magnet (h_{pm})

Following this stage, the designer must choose the stator slot type and compute the exact dimensions of the chosen stator slot type. The tooth and slot design stage of an AFPM machine has a significant impact on performance, particularly the flux distribution in the machines [1, 2, 7, 9]. Furthermore, the design of the tooth and slot is described in articles [5, 7, 8], but these articles do not mention the re-examination of the magnetic field distribution results in tooth. This article proposes a method for designing the dimensions of the stator slot for AFPM machines. The authors include thorough computation formulas, and the accuracy of the method is verified using a finite element method (FEM) simulation model.

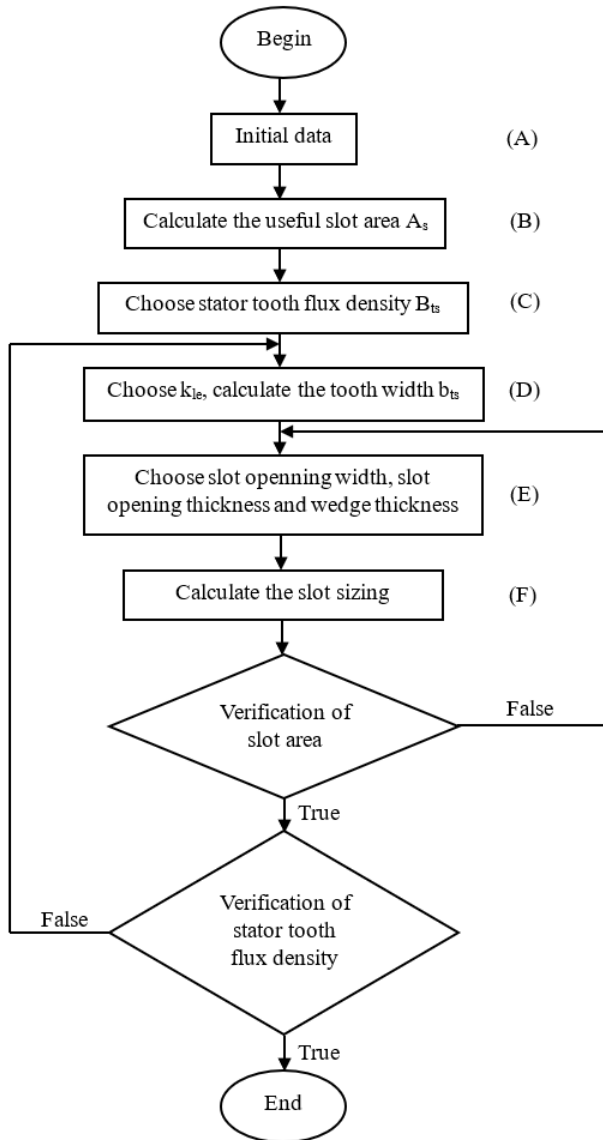


Fig. 1. The design algorithm of stator slot

2. Design Algorithm for Stator Slot of Axial Flux Permanent Magnet Machine

The algorithm diagram below depicts the precise computation processes for the design procedure of the stator slot of the AFPM machine "Fig. 1".

2.1. Detailed Design Procedures of the Algorithm

2.1.1. Initial data (A):

Based on the required parameters of the design problem and the estimated intermediate values [6]: Rated output power (S_n), rated output voltage (U_n), power factor ($\cos\phi$), linear current density (A_m), number of phases (m_1), stator outside diameter (D), ratio of inside diameter and outside diameter (k_d), current density (j).

Determine the current value of the stator.

$$I_a = \frac{S_n}{\sqrt{3}U_n} \quad (1)$$

The number of turns per phase of each stator (N_1) [1]

$$N_1 = \frac{A_m \pi D (1+k_d)}{4\sqrt{2}m_1 I_a} \quad (2)$$

The magnetic wire cross section A_w

$$A_w = \frac{I_a}{j} \quad (3)$$

2.1.2. The useful slot area A_s (B):

The required area of the slot A_s to fit the number of conductors per slot, the main wall insulation, the coil separator insulation, and the occupied area of the wedge may all be calculated using the preceding computing data.

From there, calculate the useful slot area [2]

$$A_s = \frac{A_w n_s}{k_{fill}} \quad (4)$$

Where: k_{fill} is the slot fill factor.

n_s is the number of conductors per slot

$$n_s = \frac{N_1}{p \cdot q} \quad (5)$$

Where: p is the number of poles

q is the number of slot per phase per pole

2.1.3. Select of slot type and tooth flux density of stator B_{ts} (C)

Figure 2 depicts the geometry of typical slot shapes used in rotating machines.

These geometries can be classified into two categories, one with non-parallel slot side and the other with parallel slot side. The flux lines in the 2D model of the radial flux permanent magnet (RFPM) machine are perpendicular to the rotation shaft "Fig. 3". To assure uniform tooth flux density, tooth sides must be parallel to one another, which has resulted in RFPM machine slot designs with non-parallel side structures. [2].

For the AFPM machine with a disc structure, the flux lines are in the surface parallel to the rotation shaft "Fig. 4", which is also an essential distinction from RFPM. To ensure uniform tooth flux density, the tooth sides must be parallel, resulting in slot designs for AFPM machines that are frequently oriented toward parallel side slot structures. [1].

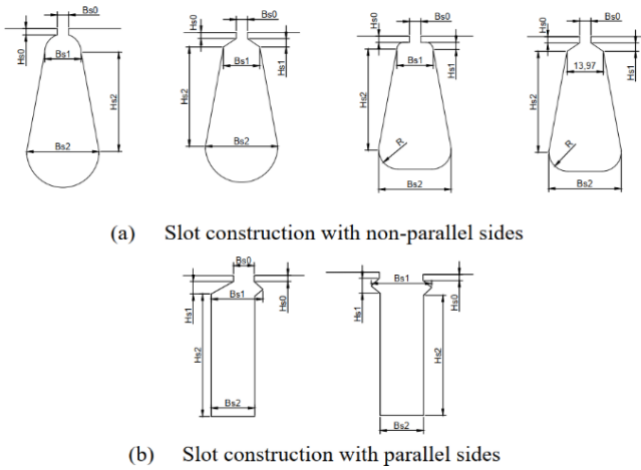


Fig. 2. Geometric structure of typical slot shapes

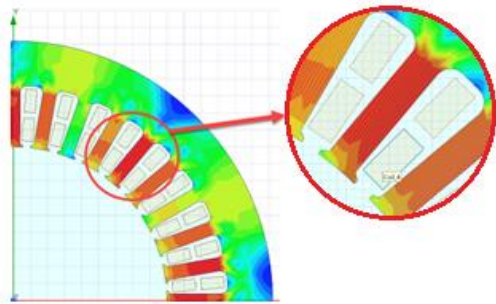


Fig. 3. Slot construction for RFPM machine with non-parallel sides

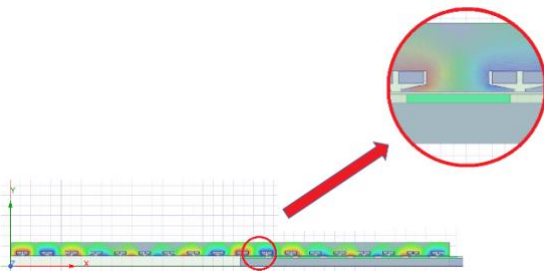


Fig. 4. Slot construction for AFPM machine with parallel sides

The article utilizes M800-50A steel with a B-H curve depicted in "Fig. 5".

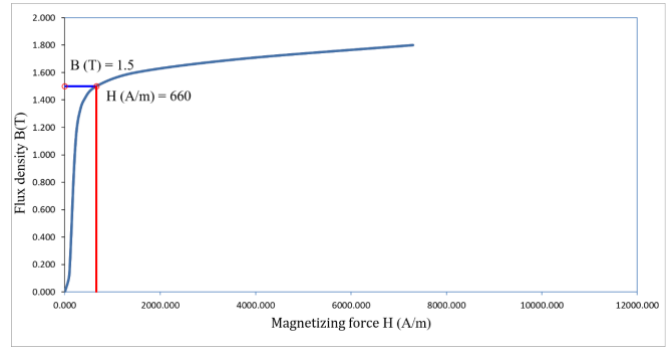


Fig. 5. B-H curve of M800-50A steel

Select the working point of the steel at point a on the magnetization curve "Fig. 5" when the machine is working at full load. At this point, the stator tooth flux density has a value of $B_{ts} = 1.5$ (T) and magnetizing force has a value of $H_{ts} = 660$ (A/m).

2.1.4. The stator tooth width b_{ts} (D):

In the main dimension determination [6], the air gap flux density (B_g) and stator slot pitch (τ_s) are computed.

Considering the d-axis, the majority of the magnetic flux generated by the magnet passes through the air gap to create the flux linkage. A small portion of the magnetic flux that does not contribute to the flux linkage is the flux leakage, which has a leakage factor of k_{le} . This coefficient is typically less than one and is dependent on the stator pole shoes "Fig. 6". Determining the stator tooth width is accomplished as follows.

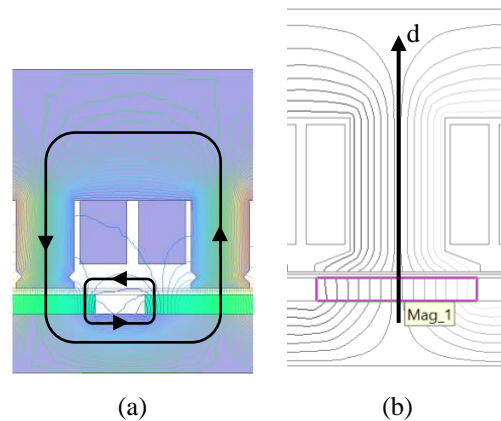


Fig. 6. Flux leakage in AFPM (a) and d-axis of magnet (b)

$$b_{ts} = \frac{k_{le} B_g \tau_s}{B_{ts} k_{Fe}} \quad (6)$$

Where: k_{Fe} is the stacking factor of stator steel

2.1.5. Detailed calculation of the dimensions of the stator slot (E):

For parallel-sided slot construction, AFPM machines typically use the slot depicted in "Fig. 7".

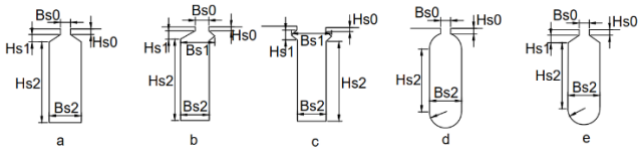


Fig. 7. Slot construction with parallel sides

Tooth width of the AFPM machine varies along the radial orientation of the stator, with the smallest width corresponding to the inner diameter d and the largest width corresponding to the outer diameter D . According to [1, 6], design parameters of the 2D model are computed using the surface corresponding to the average diameter D_{tb} "Fig. 8".

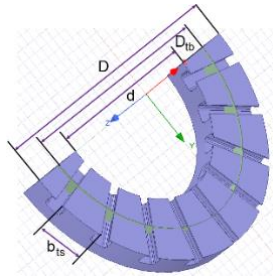


Fig. 8. Average diameter of stator

In the process of estimating the detailed dimensions of the stator slot, parameters such as slot opening B_{s0} , slot opening height H_{s0} , wedge width B_{s1} and wedge height H_{s1} , slot body bottom fillet R are typically pre-selected and adjusted when calculating the stator leakage inductances of AFPM machine [1, 2].

From the detailed slot structures shown in "Fig. 7", the following slot parameters must be determined: B_{s2} and H_{s2} .

2.1.6. Determine the slot width B_{s2} (F):

B_{s2} stator slot width is determined by the average stator diameter (D_{tb}), the number of stator slots (Z_1), and the stator tooth width (b_{ts}).

$$B_{s2} = \frac{\pi D_{tb}}{Z_1} - b_{ts} \quad (7)$$

Where:

$$D_{tb} = \frac{D+d}{2}$$

2.1.7. Determine the stator slot height H_{s2} (F cont.):

The authors develop formulas for the stator slot height "Table 2." based on the initial data and slot width (B_{s2}) computed above.

3. Simulation and Verifying Design Results

In section II, apply design algorithms and computation procedures. The simulation results of the magnetic field distribution in the tooth of the AFPM generator are as follows:

3.1. Slot type 1 "Fig. 7a"

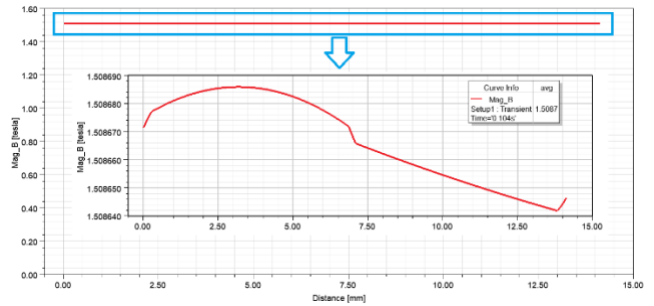
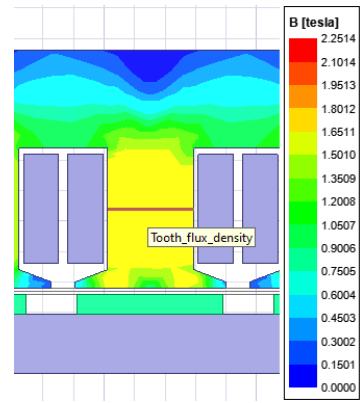


Fig. 9. Verification of design results using simulation of flux density in tooth

In the case of slot type 1, the average stator tooth flux density is $B_{avg} = 1.5087$ (T) (deviation: -0.58%) (See "Fig. 9").

3.2. Slot type 2 "Fig. 7b"

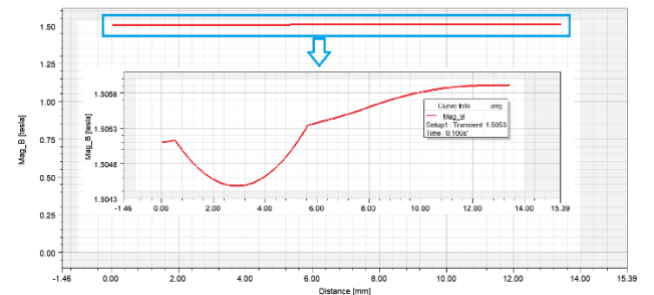
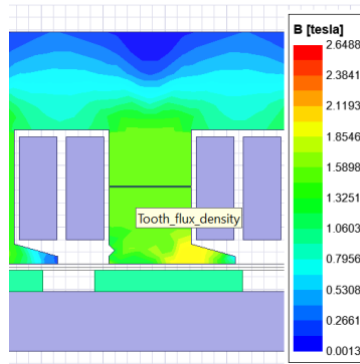


Fig. 10. Verification of design results using simulation of flux density in tooth

In the case of slot type 2, the average stator tooth flux density is $B_{avg} = 1.5053$ (T) (deviation: -0.35%) (See "Fig. 10")

3.3. Slot type 3 "Fig. 7c"

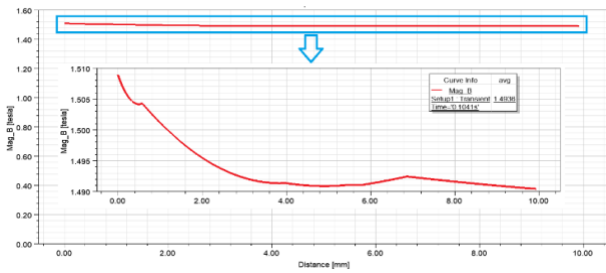
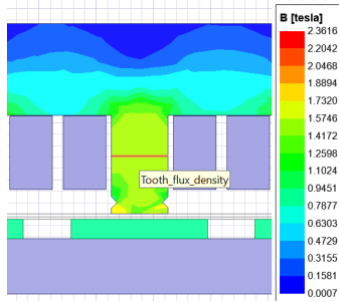


Fig. 11. Verification of design results using simulation of flux density in tooth

In the case of slot type 3, the average stator tooth flux density is $B_{avg} = 1.4936$ (T) (deviation: 0.43%). (See "Fig. 11").

3.4. Slot type 4 "Fig. 7d"

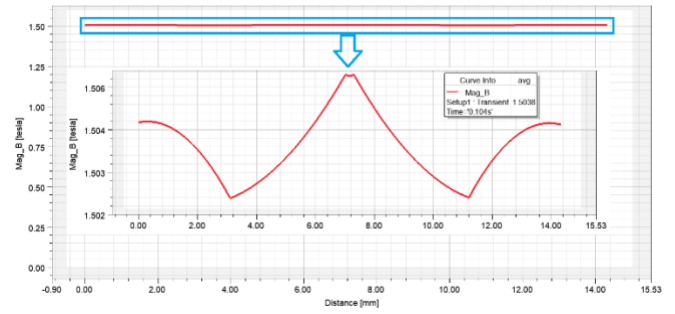
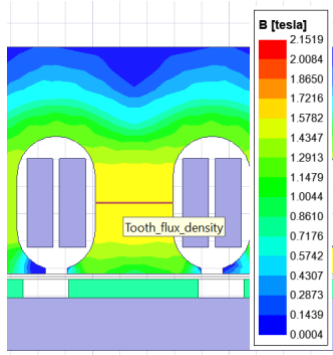


Fig. 12. Verification of design results using simulation of flux density in tooth

In the case of slot type 4, the average stator tooth flux density is $B_{avg} = 1.5038$ (T) (deviation: -0.25%). (See "Fig. 12").

3.5. Slot type 5 "Fig. 7e"

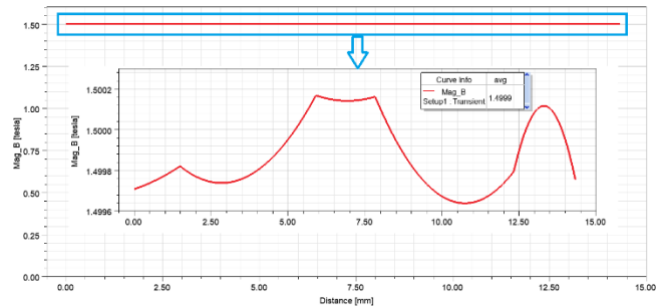
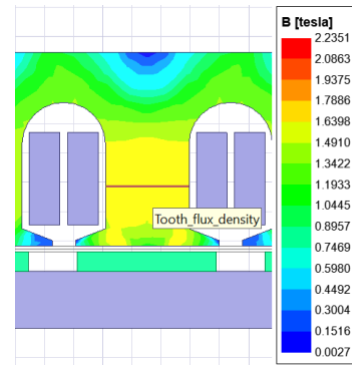


Fig. 13. Verification of design results using simulation of flux density in tooth

In the case of slot type 5, the average stator tooth flux density is $B_{avg} = 1,4998$ (T) (deviation: 0.06%). (See "Fig. 13")

Table 2. Formulas for computation of the stator slot height H_{s2}

Slot type	The stator slot height H_{s2}
Type 1 "Fig. 7a"	$H_{s2} = \frac{A_s - \frac{(B_{s0} + B_{s2})H_{s1}}{2}}{B_{s2}} \quad (8)$

Type 2 "Fig. 7b"	$H_{s2} = \frac{2A_s - (B_{s2} + B_{s0})H_{s1} - H_{s1}(B_{s1} - B_{s2})}{2B_{s2}} \quad (9)$
Type 3 "Fig. 7c"	$H_{s2} = \frac{A_s - B_{s2}H_{s1} - H_{s1}(B_{s1} - B_{s2})}{B_{s2}} \quad (10)$
Type 4 "Fig. 7d"	$H_{s2} = \frac{A_s - \frac{\pi B_{s2}^2}{4}}{B_{s2}} \quad (11)$
Type 5 "Fig. 7e"	$H_{s2} = \frac{A_s - \frac{\pi B_{s2}^2}{8} - \frac{(B_{s2} + B_{s0})H_{s1}}{2}}{B_{s2}} \quad (12)$

Table 3. Design specifications

Pre-selected parameters	Slot				
	Type 1 "Fig. 7a"	Type 2 "Fig. 7b"	Type 3 "Fig. 7c"	Type 4 "Fig. 7d"	Type 5 "Fig. 7e"
H _{s0} (mm) [1, 2]	1	1	1	1	1
H _{s1} (mm) [1, 2]	2	2	2	2	2
B _{s0} (mm) [1, 2]	4	0.5B _{s2}	B _{s2}	4	4
Computation parameters	Type 1 "Fig. 7a" Use "Eq. (8)"	Type 2 "Fig. 7b" Use "Eq. (9)"	Type 3 "Fig. 7c" Use "Eq. (10)"	Type 4 "Fig. 7d" Use "Eq. (11)"	Type 5 "Fig. 7e" Use "Eq. (12)"
B _{s1} ; B _{s2} (mm)	14.4	15.2	18.7	14.3	14.3
H _{s2} (mm)	19.9	18.5	14.3	10.2	14.5

Table 4. Design specifications (cont.)

Initial data	Value	Unit	Note
Rated power (S _n)	1	kVA	
Rated voltage (U _n)	56	V	
Outer diameter (D)	345	mm	
Inner diameter (d)	207	mm	
Length (L)	39.08	mm	

Number of slots	18	-	
Number of poles (p)	16	-	
Air gap flux density (B_g)	0.75	T	
The linear current density (A_m)	32500	A/m	
Choose current density (j)	5	A/mm ²	
Teeth flux density (B_{ts})	1.5	T	
Computation parameters			
Stator current (I_a)	10.3	A	Use "Eq. (1)"
Number of turns per phase of each stator (N_1)	163	Turn	Use "Eq. (2)"
The magnetic wire cross section (A_w) (including insulation)	2.27	mm ²	Use "Eq. (3)"
Useful slot area (A_s)	306.42	mm ²	Use "Eq. (4)"
The number of conductors per slot (ns)	54	conductor	Use "Eq. (5)"

4. Conclusion

The purpose of this article is to provide a complete design algorithm for the stator slot size of axial flux permanent magnet machines, with the authors' main contribution being to give formulae to compute the slot height H_{s2} (see Table II). The detailed computed dimensions are used to apply to several different slot types of a stator AFPM machine with the same power while maintaining the required average tooth flux density of 1.5T. When compared to the average flux density determined by the software using the finite element method, the average values computed by analysis in each of the five cases have a pretty good level of accuracy (the greatest deviation is -0.58%). The results reveal that the algorithm and formula for estimating the height of the slot H_{s2} provided by the authors have good reliability.

Acknowledgments

This research is funded by Hanoi University of Science and Technology (HUST) under project number T2022-PC-008

References

- [1] Jacek F. Gieras, Rong-Jie Wang and Maarten J. Kamper, Axial Flux Permanent Magnet Brushless Machines. Springer Science, 2008. (Book)
- [2] Juha Pyrhonen, Tapani Jokinen and Valeria Hrabovcova, Design of rotating electrical machines. John Wiley & Sons, Ltd, 2014. (Book)
- [3] Ziaul Islam, Faisal Khan, Basharat Ullah, Ahmad H. Milyani and Abdullah Ahmed Azhari, " Design and Analysis of Three Phase Axial Flux Permanent Magnet Machine with Different PM Shapes for Electric Vehicles" Energies, MDPI, 2 October 2022, doi: <https://doi.org/10.3390/en15207533>. (Article)
- [4] Zhuo Hao, Yangyang Ma, Pengyu Wang, Geng Luo and Yisong Chen, "A Review of Axial-Flux Permanent-Magnet Motors: Topological Structures, Design, Optimization and Control Techniques" Machines, MDPI, 7 December 2022, doi: <https://doi.org/10.3390/machines10121178>. (Article)
- [5] Ozturk Tosun and Necibe Fusun Oyman Serteller, "The Design of the Outer-Rotor Brushless DC Motor and an Investigation of Motor Axial-Length-to-Pole-Pitch Ratio" Sustainability 2022, 14, 12743, doi: <https://doi.org/10.3390/su141912743>. (Article)
- [6] Byung-oh tak and Jong-suk ro, "Analysis and Design of an Axial Flux Permanent Magnet Motor for in-Wheel System Using a Novel Analytical Method Combined with a Numerical Method " IEEE Access, Volume 8, November 19, 2020, doi: 10.1109/ACCESS.2020.3036666. (Article)

- [7] Werner Jara, Juan A. Tapia, Nicola Bianchi, Juha Pyrhönen, and R. Wallace "Procedure for Fast Electromagnetic Design of Axial Flux Permanent Magnet Machines " International Conference on Electrical Machines. ICEM 2014, 02-05 September 2014, doi: 10.1109/ICELMACH.2014.6960364 (Conference Paper)
- [8] Carunaiselvane and Jeevananthan, "Generalized Procedure for BLDC Motor Design and Substantiation in MagNet 7.1.1 Software " International Conference on Computing, Electronics and Electrical Technologies. ICCEET 2012, 21-22 March 2012, doi: 10.1109/ICCEET.2012.6203783 (Conference Paper)
- [9] Asko Parviainen, Design of axial-flux permanent-magnet low-speed machines and performance comparison between radial-flux and axial-flux machines, Lappeenranta University of Technology, 2005. (Thesis for the degree of Doctor).